Proposed method for molecular optical imaging

E. Betzig

NSOM Enterprises, 17 Webster Drive, Berkeley Heights, New Jersey 07922

Received September 20, 1994

We can resolve multiple discrete features within a focal region of m spatial dimensions by first isolating each on the basis of $n \geq 1$ unique optical characteristics and then measuring their relative spatial coordinates. The minimum acceptable separation between features depends on the point-spread function in the $(m + n)$-dimensional space formed by the spatial coordinates and the optical parameters, whereas the absolute spatial resolution is determined by the accuracy to which the coordinates can be measured. Estimates of each suggest that near-field fluorescence excitation microscopy/spectroscopy with molecular sensitivity and spatial resolution is possible.

The power of optical microcharacterization methods provides a strong incentive to seek means whereby they can be extended beyond the $\lambda/2$ limit of diffraction. One approach, near-field scanning optical microscopy (NSOM),[1] uses an illuminated subwavelength-sized aperture to generate a super-resolution image. As with other scanning optical techniques, spatial resolution is determined by the volume from which optical information is collected.

Here an alternative approach is proposed in which multiple discrete features within the same focal volume are spatially resolved in two steps (see Fig. 1). First, each feature is identified and isolated through one or more distinguishing optical characteristics. Second, each feature is localized; that is, its spatial coordinates are determined, on a scale that is small compared with the focal volume, either by measurement of the center of the point-spread function (PSF) associated with each feature[2] or by application of a spatial gradient,[3,4] as discussed below. The complete set of coordinates for all features can then be used to reconstruct the final image in which the relative positions of the features are shown.

The first of these steps, isolation, was recently accomplished for a spatially dense set of discrete sites of exciton recombination in a GaAs/AlGaAs single quantum well by use of cryogenic near-field microscopy/spectroscopy.[5] In general, the degree of isolation that is possible depends on the sharpness of the PSF in the entire $(m + n)$-dimensional space of m spatial coordinates and n optical parameters. Thus as the spatial resolution degrades, more sites are sampled at once, requiring increased spectral resolution to identify them all uniquely. In addition, successful isolation requires a mean volume per feature in $m + n$ space larger than the $(m + n)$-dimensional PSF. Consequently it is important to specify not only the absolute spatial resolution, which is determined by the accuracy to which the relative spatial coordinates of two distinct features can be measured, but also the minimum mean separation between features acceptable in $m + n$ space, which is dictated by the $(m + n)$-dimensional PSF.

We now consider applying the proposed method to molecular resolution fluorescence microscopy. Possibly the best path to this goal is to combine the high spatial resolution of NSOM with the high spectral resolution of cryogenic fluorescence excitation spectroscopy.[6] This reduces the minimum mean separation acceptable for isolation, improves the absolute spatial resolution by minimizing the spatial PSF used in localization, and greatly reduces photostability and background noise problems associated with far-field single-molecule detection (SMD) under ambient conditions. Several recent experiments permit the feasibility of this approach to be addressed in depth.

We first consider isolation. A normalized spectral PSF can be defined by the zero phonon absorption linewidth ν_0, as observed in single-molecule spectroscopy,[6–8] divided by the inhomogeneous linewidth ν_σ from the entire ensemble of molecules. For terrylene molecules in disordered polyethylene (Tr/PE),[9] $\nu_0 \sim 100$ MHz and $\nu_\sigma \sim 10$ THz. With a mean spectral separation 10 times larger than ν_0 to ensure isolation, this suggests that $>10^4$ molecules can be distinguished in a given focal region.

At least three limitations affect this analysis. The first is the onset of delocalization of the electronic excitation as the molecules become spatially and spectrally more dense.[9,10] Qualitatively, each excitation will remain localized to a single molecule as long as the mean dipole–dipole interaction energy between molecules[11] is small compared with the energy difference between their respective eigenvalues, i.e.,

$$\frac{p_1 p_2}{(2\pi)^2 r^3} \int_0^{2\pi} \int_0^{2\pi} |\cos(\theta_1 - \theta_2) - 3 \cos \theta_1 \cos \theta_2| \times \mathrm{d}\theta_1 \mathrm{d}\theta_2 \approx \frac{0.98 p_1 p_2}{r^3} \ll h\Delta\nu\,, \quad (1)$$

where p_1, p_2 are the molecular dipole moments, r is their spatial separation, and $\Delta\nu$ is their separation in frequency.

In the limit for which the system is homogeneous or else inhomogeneous only on a macroscopic length scale, $\Delta\nu \approx \nu_0$. This yields $r > 20$ nm for pentacene molecules in the crystalline host p-terphenyl (Pc/pTP), which is in fair agreement with photon-echo measurements.[10] It also indicates a limit to the minimum mean separation that is well short of the

0146-9592/95/030237-03$6.00/0

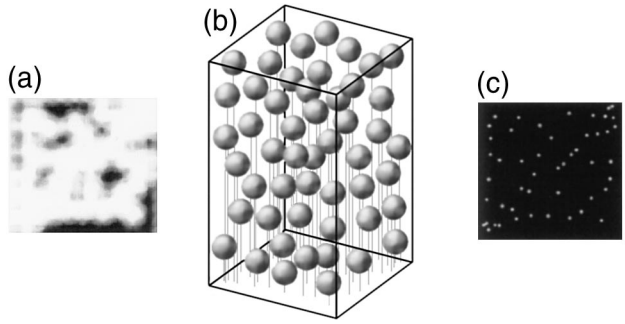

Fig. 1. (a) Field of discrete features as conventionally imaged in m spatial dimensions with a broad PSF. (b) Same features after isolation in $m + n$ dimensions on the basis of n distinguishing optical characteristics. (c) Final image reconstructed at resolution $\delta\mathbf{x}$ given by the uncertainty in the measured position of each isolated feature. In general, $|\delta\mathbf{x}| \ll$ PSF.

goal of molecular spatial resolution, although such systems might be used to explore delocalization at the level of a single molecular pair. In the opposite case of microscopic inhomogeneous broadening in which the energies between adjacent molecules are not well correlated, $\Delta\nu \sim \langle\Delta\nu\rangle_{\mathrm{tot}}$, the mean spectral separation between molecules as averaged over the entire ensemble. For a Gaussian distribution we have

$$\langle\Delta\nu\rangle_{\mathrm{tot}} = \frac{1}{\pi\nu_\sigma{}^2}\int_{-\infty}^{\infty}\int_{-\infty}^{\infty}\exp\left[-\frac{(\nu_1-\overline{\nu})^2}{\nu_\sigma{}^2}\right] \times \exp\left[-\frac{(\nu_2-\overline{\nu})^2}{\nu_\sigma{}^2}\right]|\nu_1-\nu_2|\mathrm{d}\nu_1\mathrm{d}\nu_2 \approx 0.80\nu_\sigma\,. \quad (2)$$

To reach the molecular level ($r \sim 1$ nm), relations (1) and (2) yield $\nu_\sigma \gg 180$ GHz. Microscopic inhomogeneous broadening on this scale is likely to occur in a highly disordered host such as Tr/PE.

The second limitation, which is of importance in such hosts, is spontaneous spectral diffusion and light-induced spectral shifts[12] of certain molecules within the ensemble. However, Stark coefficients for Tr/PE are independent of spectral diffusion[8] and therefore can be used to tag such molecules uniquely. In addition, excitation intensities of $I_{\mathrm{exc}} < 1$ mW/cm^2 minimize light-induced spectral shifts yet are sufficient for practical SMD.

A final complication arises from the interaction between each molecule and the aluminum coating on the NSOM probe, which can quench the signal owing to nonradiative energy transfer and also shift the molecular excitation frequency. Theoretical estimates[13] suggest that neither effect will be problematic at molecule–probe separations of >20 nm.

The spatial component of the overall PSF is determined by the diameter of the near-field aperture, which should be no larger than is needed to reach the I_{exc} at which light-induced spectral shifts becomes significant. Saturation, which requires a much larger I_{exc} (>1 W/cm^2), was recently claimed for Pc/pTP by use of an aperture of radius $a = 30$ nm.[14]

We now consider localization. The spatial coordinates $\mathbf{x}_i$ of each isolated molecule can be estimated with a quantitative uncertainty $\delta\mathbf{x}_i$ by application of a χ^2 maximum-likelihood analysis to the data by use of a known PSF, $h(\mathbf{x})$. In each spatial dimension η with N data points from $-\beta a$ to βa, it is found that[2]

$$\delta\eta = \left(\frac{\Delta}{\Omega N}\right)^{1/2}, \qquad \Omega = \frac{1}{2\beta a}\int_{-\beta a}^{\beta a}\frac{1}{\sigma^2(\eta)}\left[\frac{\partial h(\eta)}{\partial\eta}\right]^2\mathrm{d}\eta\,, \quad (3)$$

where Δ depends on the number of parameters in the fit and the desired confidence level [$\Delta = 4.61$ in Eq. (3) for 90% confidence] and $\sigma(\eta)$ is the standard measurement error at position η.

In NSOM SMD,[15] $\sigma^2(\eta) = h(\eta)$ since Poisson-distributed shot noise dominates. Furthermore we find that

$$h(\eta) = S_{\hat{p},\hat{\eta}}(z)|\hat{p}\cdot\hat{E}(\eta, z)|^2 \equiv S_{\hat{p},\hat{\eta}}(z)h_{\hat{p}}(\eta, z)\,, \quad (4)$$

where $S_{\hat{p},\hat{\eta}}(z)$ is the maximum signal (in counts) along the measured range on the $\hat{\eta}$ axis at a distance z from the plane of the aperture for a particular orientation $\hat{p}$ of the molecular dipole moment. Experiments demonstrate that the normalized electric field $\hat{E}(\mathbf{x})$ in the vicinity of the aperture is well approximated by the Bethe–Bouwkamp model,[16] in which a plane wave polarized along the x axis is incident upon an aperture with $a \ll \lambda$. Except when $\hat{p}\cdot\hat{x} = 0$, $\hat{p}\cdot\hat{z} = 0$, or $\hat{p}\cdot\hat{z} = 1$, $h_{\hat{p}}(-\eta, z) \neq \pm h_{\hat{p}}(\eta, z)$ in relation (4), and a more complicated form of Eqs. (3) is required. However, because the spatial-frequency content of $h_{\hat{p}}(\eta, z)$ does not depend strongly on $\hat{p}$, $\delta\eta_{\hat{p}}$ should always be of the same order as for these three cases. Relations (3) and (4) then yield

$$\delta\eta_{\hat{p}}(\beta, z) = \left[\frac{\Delta}{N\Psi_{\hat{p},\hat{\eta}}(\beta, z)S_{\hat{p},\hat{\eta}}(z)}\right]^{1/2}\cdot a\,, \quad (5a)$$

$$\Psi_{\hat{p},\hat{\eta}}(\beta, z) = \frac{1}{\beta}\int_0^{\beta}\frac{1}{h_{\hat{p}}(\zeta, z)}\left[\frac{\partial h_{\hat{p}}(\zeta, z)}{\partial\zeta}\right]^2\mathrm{d}\zeta, \qquad \zeta = \eta/a\,. \quad (5b)$$

Consider the problem of determining the x, y coordinates (i.e., $\eta = x$ or $\eta = y$) of two molecules oriented along the x ($\hat{p} = \hat{x}$) and z ($\hat{p} = \hat{z}$) axes, respectively. The relevant PSF's from relation (4) and the Bethe–Bouwkamp model are shown in Fig. 2, normalized to the maximum of $h_x(x, 0.2a)$. To minimize $\delta\eta$, we take each PSF along a line chosen to pass near the maximum of $h_{\hat{p}}(\mathbf{x})$. Numerical integration of Eq. (5b) leads to the curves $\Psi_{\hat{p},\hat{\eta}}(\beta, z)$ shown in Fig. 3, which can be used to calculate $\delta\eta$ according to Eq. (5a).

In each case there exists an optimum range $\pm\beta a$ over which the χ^2 fit should be performed to minimize $\delta\eta$. A good choice in all four cases is $\beta = 1.3$. By using Figs. 2 and 3, $a = 40$ nm, and $S_{\hat{p},\hat{\eta}} = 400$ counts as typical,[15] we find $\delta x_x = 0.94$ nm, $\delta y_x = 1.01$ nm, $\delta x_z = 0.62$ nm, and $\delta y_z = 1.15$ nm at $z = 0.5a = 20$ nm for $N = 10$ and $\Delta = 4.61$. These uncertainties are consistent with absolute spatial resolution on the molecular level. Furthermore such resolution can be maintained even for $z > 2a$, provided that I_{exc} is adjusted to keep $S_{\hat{p},\hat{\eta}} \sim 400$.

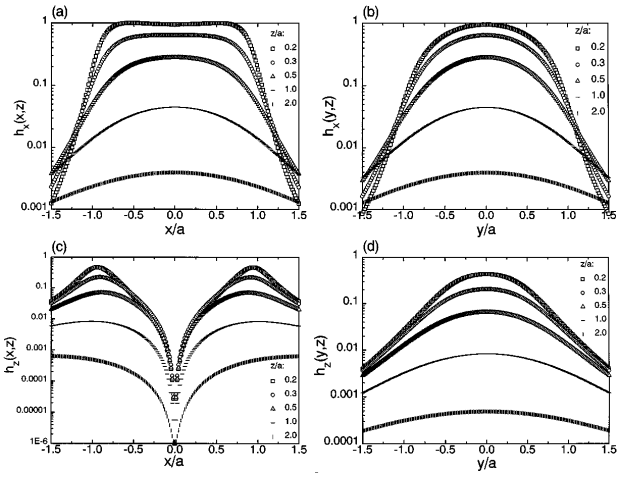

Fig. 2. PSF's $h_{\hat{p}}(\eta, z)$ along the η axis for a molecule at orientation $\hat{p}$ at a distance z from a near-field aperture of radius a: (a) $\hat{p} = \hat{x}$, $\eta = x$; (b) $\hat{p} = \hat{x}$, $\eta = y$; (c) $\hat{p} = \hat{z}$, $\eta = x$; (d) $\hat{p} = \hat{z}$, $\eta = y$.

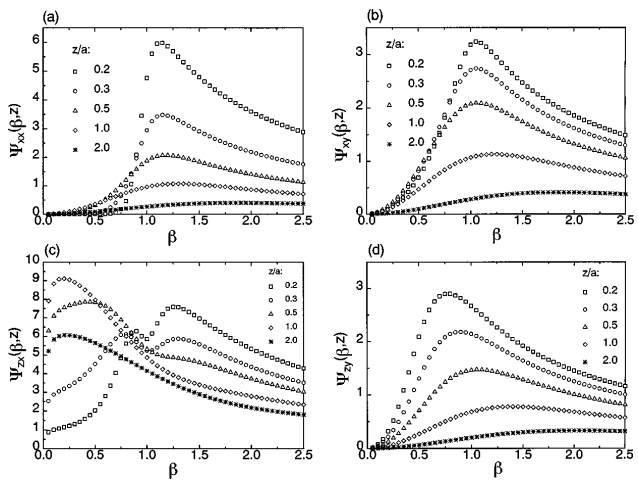

Fig. 3. Parameter $\Psi_{\hat{p},\hat{\eta}}(\beta, z)$ used to calculate the position uncertainty $\delta\mathbf{x}$ as a function of the range $2\beta a$ of the χ^2 fit [(a)–(d) correspond to the same $\hat{p}$ and η values as in Fig. 2].

One caveat is that $h_{\hat{p}}(\eta, z)$ might differ from the form given by relation (4) and the Bethe–Bouwkamp model. However, variations owing to imperfections in the aperture will vanish exponentially with increasing z, and other differences can be accounted for by measurement of the PSF on well-isolated molecules. Another caveat is that $\mathbf{x}_i$ and $\delta\mathbf{x}_i$ should ideally be determined through a six-parameter fit reflecting all the variables within the PSF (S; x, y, z; and $\hat{p} \cdot \hat{x}$, $\hat{p} \cdot \hat{z}$). However, this approach should reduce $\delta\mathbf{x}$, as it exploits all the data in the scan plane rather than just along a line, as above.

A complementary method of localization is to apply a strong spatial gradient[3,4] to which one or more of the n optical characteristics is sensitive. The resultant large separations between features in the affected optical dimensions then directly reflect minute separations in space. Consider, for example, Stark spectroscopy. By applying a 10-V potential to a NSOM probe with a 250-nm outer diameter one obtains an electric-field gradient of >10 kV/(cm nm) near the aperture, yielding a Stark shift of ~0.2–1.0 GHz/nm for Tr/PE.[8] Given $\nu_0 \sim 100$ MHz, this should lead to molecular spatial resolution. However, a sophisticated algorithm will be needed to take into account the inhomogeneous spreading at zero field and the variation in the Stark shift resulting from different molecular orientations. Alternatively, externally applied Stark shifts might be used to alter the spectral separation between adjacent molecules and thus the onset of delocalization.

In conclusion, the proposed method should be capable of near-molecular resolution in three dimensions. In conjunction with well-established fluorescence labeling techniques, it might be applied to the structural mapping of protein molecules or to gene mapping and DNA sequencing.

References

1. E. Betzig, in *Near-Field Optics*, D. W. Pohl and D. Courjon, eds. (Kluwer, Dordrecht, The Netherlands, 1993), pp. 7–15.
2. N. Bobroff, Rev. Sci. Instrum. **57,** 1152 (1986).
3. J. A. Sidles, Appl. Phys. Lett. **58,** 2854 (1991); Phys. Rev. Lett. **68,** 1124 (1992).
4. D. Rugar, C. S. Yannoni, and J. A. Sidles, Nature (London) **360,** 563 (1992); D. Rugar, O. Züger, S. Hoen, C. S. Yannoni, H. M. Vieth, and R. D. Kendrick, Science **264,** 1560 (1994).
5. H. F. Hess, E. Betzig, T. D. Harris, L. N. Pfeiffer, and K. W. West, Science **264,** 1740 (1994).
6. M. Orrit and J. Bernard, Phys. Rev. Lett. **65,** 2716 (1990); H. Talon, L. Fleury, J. Bernard, and M. Orrit, J. Opt. Soc. Am. B **9,** 825 (1992).
7. W. P. Ambrose, Th. Basché, and W. E. Moerner, J. Chem. Phys. **95,** 7150 (1991).
8. M. Orrit, J. Bernard, and A. Zumbusch, Chem. Phys. Lett. **196,** 595 (1992).
9. L. Root and J. L. Skinner, J. Chem. Phys. **81,** 5310 (1984); R. F. Loring, H. C. Anderson, and M. D. Fayer, J. Chem. Phys. **81,** 5395 (1984).
10. R. J. Gulotty, C. A. Walsh, F. G. Patterson, W. L. Wilson, and M. D. Fayer, Chem. Phys. Lett. **125,** 507 (1986).
11. J. D. Jackson, *Classical Electrodynamics*, 2nd ed. (Wiley, New York, 1975), p. 143.
12. Th. Basché and W. E. Moerner, Nature (London) **355,** 335 (1992); Th. Basché, W. P. Ambrose, and W. E. Moerner, J. Opt. Soc. Am. B **9,** 829 (1992).
13. R. R. Chance, A. Prock, and R. Silbey, Adv. Chem. Phys. **37,** 1 (1978); X. Xie, Pacific Northwest Laboratory, Richland, Wash. (personal communication, 1994).
14. W. E. Moerner, T. Plakhotnik, T. Irngartinger, U. P. Wild, D. W. Pohl, and B. Hecht, Phys. Rev. Lett. (to be published).
15. E. Betzig and R. J. Chichester, Science **262,** 1422 (1993).
16. H. A. Bethe, Phys. Rev. **66,** 163 (1944); C. J. Bouwkamp, Philips Res. Rep. **5,** 321 (1950).